11. Mathematikertreffen, Zagreb-Graz
D. Butkovič, D. Gronau,
H. Kraljevič, O. Röschel (Eds.)
Grazer Math. Ber., ISSN 1016–7692
Bericht Nr. 3xx (2005), 1-22

Effective model of the fluid flow through elastic tube with variable radius

Josip Tambača, Sunčica Čanić and Andro Mikelić

Abstract

We study the flow of an incompressible viscous Newtonian fluid through a tube with compliant walls. The tube is assumed to be straight, long, with circular cross–sections of variable radius. Elastic properties of the tube wall are described by the linear membrane shell equations. The flow is driven by the pulsatile inlet and outlet dynamic pressure data. Applying asymptotic techniques we derive a closed reduced model. The model is of mixed hyperbolic–parabolic type with memory effects. This two dimensional model can be solved as a system of two one–dimensional problems, so it has the complexity of one-dimensional problems. This provides an efficient numerical algorithm for a model that captures leading order 2–dimensional effects.

1 Introduction

This paper is motivated by the study of blood flow in compliant arteries. In medium to large vessels blood is usually modelled as an incompressible Newtonian fluid [11, 12]. The vessel walls we consider to be thin, behaving as a prestressed linearly elastic membrane shell [9, 10, 2]. The flow is driven by the inlet and outlet pressure that is periodic in time. We look for a closed, effective model that approximates the 3D problem to the ε^2–accuracy, where ε is the aspect ratio of the problem, defined in (1.1). The axially symmetric problem in the straight tube with the constant reference radius was studied in [5]. The numerical results presented in [6] show excellent agreement with the experimental data.

Here we generalize the results in [5] and [6] for the tubes with circular cross–sections of variable radius (i.e. radius R is a function of the longitudinal variable). This is the case ,for example, in tapered arteries, aneurysms or stenosis.

We first formulate the three-dimensional problem. Then we derive the a priori estimates from the energy equality of the problem. These estimates are used to define nondimensional quantities in the problem. This enables us to compare the terms in the

Mathematics Subject Classification 2000: Primary 74F10, Secondary 35Q30, 74K15.
Keywords and phrases: fluid flow, elastic tube, fluid–structure interaction, effective model.

problem and to build a simplified approximation. For straight tubes there are two basic assumptions:

$$\varepsilon = \frac{\max R}{L} \tag{1.1}$$

is small (the radius is small compared to the length of the tube) and the deflection of the tube wall is small compared to the radius. For tubes with variable radius our result is also limited by the assumption that the radius varies slowly: $R' \approx \varepsilon$ and that the first and second derivatives with respect to the spatial variables of the fluid velocity and the displacement of the structure are all of order one.

We obtain the equations that are closed and of mixed, hyperbolic–parabolic type with memory. The memory effects capture the viscoelastic nature ([1]) of the coupled fluid–structure interaction problem. We also derive a numerical algorithm for the reduced model. The algorithm uses the one–dimensional finite element method with C^1 elements for both space variables and an implicit discretization of time.

2 Setting up the problem

We study the flow of an incompressible Newtonian fluid in an axially symmetric cylindrical domain with variable radius governed by the time-dependent inlet and outlet boundary data. In the reference configuration the length of the domain is denoted by L. For a given smooth function $R : [0, L] \to \mathbb{R}$, the radius of the cylinder at $z \in [0, L]$ is denoted by $R(z)$. The reference domain is now defined by (see Figure 1)

$$\Omega = \left\{x = (r\cos\theta, r\sin\theta, z) \in \mathbb{R}^3 : r \in (0, R(z)), \theta \in (0, 2\pi), z \in (0, L)\right\}$$

and its lateral boundary is given by

$$\Sigma = \left\{x = (R(z)\cos\theta, R(z)\sin\theta, z) \in \mathbb{R}^3 : \theta \in (0, 2\pi), z \in (0, L)\right\}.$$

We assume that the domain is thin and long, i.e. the nondimensional parameter $\varepsilon = \frac{R_{\max}}{L}$

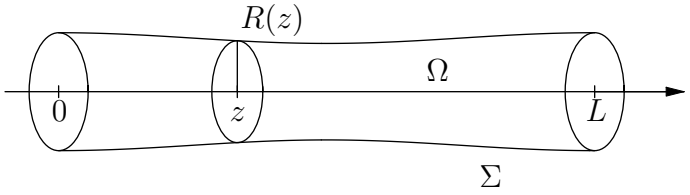

Figure 1: The reference domain

is small, where $R_{\max} = \max_{z\in[0,L]} R(z)$.

The lateral boundary is assumed to be elastic and to deform as a result of the fluid–structure interaction between the fluid and the structure. To be precise we assume that Σ behaves as a homogeneous, isotropic, linearly elastic membrane shell with thickness h [3] and that at the reference configuration the shell is prestressed by $T^0_{\theta\theta} = p_{\text{ref}}\frac{R_{\max}}{h}$,

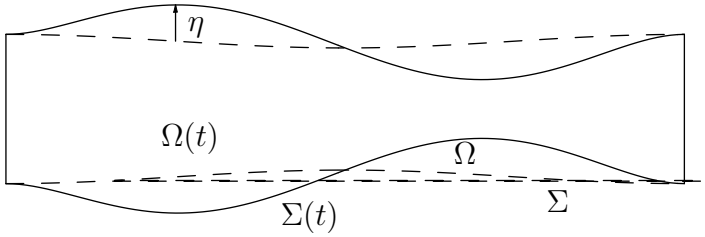

Figure 2: The deformed domain

where $T^0_{\theta\theta}$ is the θ,θ component of the stress tensor (see [9, 10]). Moreover, we account for the radial displacements η of the shell only. Therefore the strain, given by the linear part of the change of metric tensor of the shell, is given by

$$\mathbf{G}(\eta) = \frac{1}{2}\mathrm{Lin}\begin{pmatrix} (R'+\eta')^2 - (R')^2 & 0 \\ 0 & (R+\eta)^2 - R^2 \end{pmatrix} = \begin{pmatrix} R'\eta' & 0 \\ 0 & R\eta \end{pmatrix}.$$

Here $'$ denotes the derivative with respect to the longitudinal variable. Then, for a given radial component of the force f_r, the model equation for the boundary behavior in the weak formulation is given by

$$\begin{aligned} &\int_0^L h\rho_S \frac{\partial^2\eta}{\partial t^2}\xi R\sqrt{1+(R')^2}dz + \int_0^L \Big(\frac{\sigma hE}{1-\sigma^2}\left(\frac{R'}{1+(R')^2}\eta' + \frac{1}{R}\eta\right)\left(\frac{R'}{1+(R')^2}\xi' + \frac{1}{R}\xi\right) \\ &+\frac{hE}{1+\sigma}\left(\left(\frac{R'}{1+(R')^2}\right)^2\eta'\xi' + \frac{1}{R^2}\eta\xi\right)\Big)R\sqrt{1+(R')^2}dz \qquad (2.1) \\ &+\int_0^L hT^0_{\theta\theta}\frac{\eta\xi}{R^2}R\sqrt{1+(R')^2}dz = \int_0^L f_r\xi R\sqrt{1+(R')^2}dz, \qquad \xi\in H^1_0(0,L); \end{aligned}$$

here E is the Young modulus, σ the Poisson ratio, ρ_S is the shell density. For simplicity we only take the membrane part of the shell model (the Koiter shell model [2]). Note, as well, that the radial component η is not the component of the displacement normal to the shell.

With these assumptions on the geometry of the problem, the moving domain $\Omega(t)$ at time t is given by

$$\Omega(t) = \left\{(r\cos\theta, r\sin\theta, z)\in\mathbb{R}^3 : r\in(0, R(z)+\eta(t,z)), \theta\in(0,2\pi), z\in(0,L)\right\},$$

while the wall of the cylinder at time t is described by

$$\Sigma(t) = \left\{((R(z)+\eta(t,z))\cos\theta, (R(z)+\eta(t,z))\sin\theta, z)\in\mathbb{R}^3 : \theta\in(0,2\pi), z\in(0,L)\right\},$$

see Figure 2. We also denote the inlet and outlet boundary $B_0(t) = \partial\Omega(t)\cap\{z = 0\}, B_L(t) = \partial\Omega(t)\cap\{z = L\}$.

Now we search for the axially symmetric solution (v_r, v_z, η), where $\boldsymbol{v} = (v_r, v_z)$ is the fluid velocity, of the problem defined by the following:

a) the fluid satisfies the incompressible Navier–Stokes equations in $\Omega(t)$

$$\rho_F\left(\frac{\partial v_r}{\partial t}+v_r\frac{\partial v_r}{\partial r}+v_z\frac{\partial v_r}{\partial z}\right)-\mu\left(\frac{\partial^2 v_r}{\partial r^2}+\frac{\partial^2 v_r}{\partial z^2}+\frac{1}{r}\frac{\partial v_r}{\partial r}-\frac{v_r}{r^2}\right)+\frac{\partial p}{\partial r}=0,$$
$$\rho_F\left(\frac{\partial v_z}{\partial t}+v_r\frac{\partial v_z}{\partial r}+v_z\frac{\partial v_z}{\partial z}\right)-\mu\left(\frac{\partial^2 v_z}{\partial r^2}+\frac{\partial^2 v_z}{\partial z^2}+\frac{1}{r}\frac{\partial v_z}{\partial r}\right)+\frac{\partial p}{\partial z}=0,$$
$$\frac{\partial v_r}{\partial r}+\frac{\partial v_z}{\partial z}+\frac{v_r}{r}=0.$$

Here p is the pressure, μ is the fluid dynamic viscosity coefficient and ρ_F is the fluid density;

b) the moving boundary $\Sigma(t)$ behaves as the linearly membrane shell defined by the equations (2.1);

c) the kinematic condition on the contact $\Sigma(t)$ of the fluid and the structure is the continuity of the velocity

$$v_r(R+\eta(z,t),z,t)=\frac{\partial\eta(z,t)}{\partial t},\quad v_z(R+\eta(z,t),z,t)=0;$$

d) the dynamic condition on the contact $\Sigma(t)$ of the fluid and the structure is the continuity of the contact force. Since the radial component of the fluid contact force $[(p-p_{\rm ref})\mathbf{I}-2\mu D(\boldsymbol{v})]\,\boldsymbol{n}\cdot\boldsymbol{e}_r$ is given in the Eulerian coordinates, where $p_{\rm ref}$ is the reference pressure, and the structure contact force (2.1) is given in the Lagrangian coordinates, we must take into account the Jacobian of the transformation from the Eulerian to the Lagrangian coordinates $J:=\sqrt{\det((\nabla\boldsymbol{\phi})^T\nabla\boldsymbol{\phi})}=\sqrt{(R+\eta)^2\,(1+(R'+\eta')^2)}$, where $\boldsymbol{\phi}:(z,\theta)\mapsto(x,y,z)$ and its gradient $\nabla\boldsymbol{\phi}$ are defined by

$$\begin{array}{l}x=(R+\eta)\cos\theta\\ y=(R+\eta)\sin\theta\\ z=z\end{array},\quad \nabla\phi=\begin{pmatrix}(R'+\eta')\cos\theta & -(R+\eta)\sin\theta\\ (R'+\eta')\sin\theta & (R+\eta)\cos\theta\\ 1 & 0\end{pmatrix}.$$

Here $\boldsymbol{n}$ is the unit normal at the deformed structure

$$\boldsymbol{n}=-\frac{R'+\eta'}{\sqrt{1+(R'+\eta')^2}}\boldsymbol{e}_z+\frac{1}{\sqrt{1+(R'+\eta')^2}}\boldsymbol{e}_r.$$

The coupling is then performed by requiring that for every Borel subset B of the lateral boundary Σ, the contact force exerted by the fluid to the structure equals, but is of opposite sign to the contact force exerted by the structure to the fluid, namely,

$$\int_B[(p-p_{\rm ref})\mathbf{I}-2\mu D(\boldsymbol{v})]\,\boldsymbol{n}\cdot\boldsymbol{e}_r J d\theta dz=\int_B f_r R\sqrt{1+(R')^2}d\theta dz$$

and so, pointwise, the dynamic coupling condition reads

$$[(p-p_{\rm ref})\mathbf{I}-2\mu D(\boldsymbol{v})]\,(-(R'+\eta')\boldsymbol{e}_z+\boldsymbol{e}_r)\cdot\boldsymbol{e}_r\left(1+\frac{\eta}{R}\right)\frac{1}{\sqrt{1+(R')^2}}=f_r, \quad (2.2)$$

where f_r is given in (2.1).

e) boundary conditions (inlet/outlet conditions)

$$v_r=0,\ \ p+\rho_F(v_z)^2/2=P_0(t)+p_{\rm ref} \quad \text{on} \quad B_0(t), \quad (2.3)$$
$$v_r=0,\ p+\rho_F(v_z)^2/2=P_L(t)+p_{\rm ref} \quad \text{on} \quad B_L(t), \quad (2.4)$$
$$\eta=0 \ \text{ for } \ z=0, \quad \eta=0 \ \text{ for } \ z=L \ \text{ and } \forall t\in\mathbb{R}_+, \quad (2.5)$$

for P_0, P_L given functions of t only.

f) initial conditions

$$\eta=\frac{\partial\eta}{\partial t}=0 \quad \text{and} \quad \boldsymbol{v}=0 \quad \text{on} \quad \Sigma\times\{0\}. \quad (2.6)$$

The problem defined by a)–f) is a three–dimensional fluid–structure interaction problem. It is the starting point for our analysis.

The assumption of zero longitudinal displacement of the structure leads to a limited applicability of the model in the case of tube with variable radius of the cross–section. Still, we believe that for a small change of the radius the model is reasonable.

The flow is driven by the inlet/outlet time dependent dynamic pressure. In the simplified model this condition reduces to requiring only the pressure which can be measured. As a consequence, a boundary layer forms to compensate the zero displacement of the structure and the displacement forced by the inlet/outlet pressure. In [4] it was proved that boundary layer affects the flow around inlet/outlet only locally.

In the next section we derive the a priori estimates for the velocity and the displacement from the total energy of the problem. These estimates lead to the nondimensional equations of the problem from which we deduce the reduced model.

3 The a priori estimates

The main step in the derivation of the effective equations approximating the problem a)–f) are the a priori estimates. These estimates provide the magnitudes of the unknown functions in the problem $\boldsymbol{v}, p, \eta$ which we use to write the nondimensional equations.

We start with the energy equality. The Navier–Stokes equations are multiplied by the velocity and integrated over the space domain $\Omega(t)$. Then after integration by parts and application of the boundary and contact conditions we obtain the following Lemma.

Lemma 3.1 *Solution $(\boldsymbol{v},\eta)$ satisfies the following energy equality*

$$\frac{\rho_F}{2}\frac{d}{dt}\int_{\Omega(t)}\boldsymbol{v}^2dV+2\mu\int_{\Omega(t)}D(\boldsymbol{v})\cdot D(\boldsymbol{v})dV+\frac{d}{dt}\int_0^L h\rho_S\left(\partial_t\eta\right)^2\pi R\sqrt{1+(R')^2}dz$$
$$+\frac{d}{dt}\int_0^L\left(\frac{\sigma hE}{1-\sigma^2}\left(\frac{R'\eta'}{1+(R')^2}+\frac{\eta}{R}\right)^2+\frac{hE}{1+\sigma}\left(\left(\frac{R'\eta'}{1+(R')^2}\right)^2+\frac{\eta^2}{R^2}\right)\right)\pi R\sqrt{1+(R')^2}dz$$
$$+\frac{d}{dt}\int_0^L hT^0_{\theta\theta}\frac{\eta^2}{R^2}\pi R\sqrt{1+(R')^2}dz=\int_{B_0(t)}v_zP_0(t)dS-\int_{B_L(t)}v_zP_L(t)dS \tag{3.1}$$

Now we rescale time by introducing the nondimensional time $\overline{t}=\omega t$, where ω is the characteristic frequency, which will be specified later in (3.3). To simplify notation we keep t to denote the rescaled time until section 4.1. We also denote

$$Q=\left(T^0_{\theta\theta}+\frac{E}{1+\sigma}\right)\frac{h}{R},\qquad Q_{\min}=\min Q\qquad R_{\min}=\min R,\qquad R_{\max}=\max R.$$

To obtain the a priori estimates we integrate (3.1) over time, use the initial conditions, estimate the left–hand side from below and take only the η^2 term from the potential energy of the membrane to obtain

$$\frac{\rho_F\omega}{2}\|\boldsymbol{v}\|^2_{\Omega(t)}+2\mu\int_0^t\|D(\boldsymbol{v})\|^2_{\Omega(\tau)}d\tau+\rho_S\omega^3\pi hR_{\min}\int_0^L\left(\partial_t\eta\right)^2dz+\omega\pi Q_{\min}\int_0^L\eta^2dz$$
$$\leq\int_0^t\left(\int_{B_0(t)}v_zP_0(t)dS-\int_{B_L(t)}v_zP_L(t)dS\right)d\tau. \tag{3.2}$$

In the sequel we estimate the right–hand side using the terms on the left–hand side. Functions

$$\hat{p}(t)=\frac{A(t)}{L}z+P_0(t),\qquad A(t)=P_L(t)-P_0(t)$$

and the Green formula applied to the right–hand side allow us to write

$$\begin{aligned}&\int_0^t\left(\int_{B_L(\tau)}v_zP_L(\tau)dS-\int_{B_0(\tau)}v_zP_0(\tau)dS\right)d\tau\\&=\int_0^t\left(\int_{\Omega(\tau)}\operatorname{div}\left(\hat{p}\boldsymbol{v}\right)dS-\int_{\Sigma(\tau)}\hat{p}\boldsymbol{v}\cdot\boldsymbol{\nu}d\Sigma(\tau)\right)d\tau\\&=\int_0^t\left(\int_{\Omega(\tau)}\frac{A(\tau)}{L}v_zdS-\int_0^L\int_0^{2\pi}\hat{p}\omega\partial_\tau\eta\nu_rJ\right)d\theta dzd\tau\end{aligned}$$

where $\nu_r=\frac{R+\eta}{\sqrt{(R+\eta)^2(1+(R'+\eta')^2)}}$ and $J=\sqrt{(R+\eta)^2(1+(R'+\eta')^2)}$ are the radial component of the unit normal on Σ and the Jacobian of the change of coordinates. The last two terms we estimate separately.

Lemma 3.2 *For any $\alpha > 0$ one has*

$$\begin{aligned}
&\left|2\pi\omega\int_0^t\int_0^L \hat{p}\frac{\partial\eta}{\partial t}(R+\eta)dzd\tau\right| \\
&\leq \frac{8\pi R_{\max}^2\omega}{Q_{\min}}\int_0^L \hat{p}^2dz + \frac{\pi\omega Q_{\min}}{8}\|\eta\|^2 + \frac{8\pi\omega L R_{\max}^2}{Q_{\min}}\left(\sup_z\int_0^t|\partial_t\hat{p}|d\tau\right)^2 \\
&\quad + \frac{\pi\omega Q_{\min}}{8L}L\sup_t\|\eta\|^2 + \pi\omega\frac{\|\hat{p}\|_\infty^2}{\alpha Q_{\min}}\int_0^t\left\|\frac{\partial\eta}{\partial t}\right\|^2 + \pi\omega\alpha Q_{\min}\int_0^t\|\eta\|^2
\end{aligned}$$

Proof. The coefficient in (3.2) in front of η^2 is much greater than the coefficient in front of $\partial_t\eta$. Therefore we integrate by parts to remove the time derivative from η.

$$\begin{aligned}
&\left|2\pi\omega\int_0^t\int_0^L \hat{p}\frac{\partial\eta}{\partial t}(R+\eta)dzd\tau\right| = 2\pi\omega\left|\int_0^t\int_0^L R\hat{p}\frac{\partial\eta}{\partial t} + 2\pi\omega\int_0^t\int_0^L\hat{p}\frac{\partial\eta}{\partial t}\eta\right| \\
&= \left|2\pi\omega\int_0^t\int_0^L R\frac{\partial}{\partial t}(\hat{p}\eta) - 2\pi\omega\int_0^t\int_0^L R\frac{\partial\hat{p}}{\partial t}\eta + 2\pi\omega\int_0^t\int_0^L\hat{p}\frac{\partial\eta}{\partial t}\eta\right| \\
&\leq \pi\omega R_{\max}^2\frac{8}{Q_{\min}}\left|\int_0^L\hat{p}^2dz\right| + \frac{\pi\omega Q_{\min}}{8}\left|\int_0^L\eta^2dz\right| \\
&\quad + 2\pi\omega\left(\sqrt{\frac{8LR_{\max}}{Q_{\min}}}\sup_z\int_0^t|\partial_t\hat{p}|d\tau\right)\left(\sqrt{\frac{R_{\max}Q_{\min}}{8L}}\sup_t\int_0^L\eta dz\right) \\
&\quad + 2\pi\omega\int_0^t\int_0^L\left(\sqrt{\frac{1}{\alpha Q_{\min}}}\hat{p}\frac{\partial\eta}{\partial t}\right)\left(\sqrt{\alpha Q_{\min}}\eta\right).
\end{aligned}$$

The estimate follows by applying the inequality $2ab \leq a^2+b^2$ and the Schwartz–Cauchy inequality several times. □

Lemma 3.3 *Let $\frac{\|A\|_\infty^2}{\rho_F L^2} \leq \frac{\|\hat{p}\|_\infty^2}{\rho_S h R_{\min}}$. Then for any $\alpha > 0$ one has*

$$\begin{aligned}
\left|\int_0^t\int_{\Omega(t)}\frac{A(t)}{L}v_z d\boldsymbol{x}d\tau\right| &\leq \frac{\rho_F\alpha\omega}{2}\int_0^t\|v_z\|_{\Omega(\tau)}^2d\tau + \frac{\pi}{\rho_F\alpha\omega L^2}R^2L\int_0^t|A(\tau)|^2d\tau \\
&\quad + \frac{\pi\|\hat{p}\|_\infty^2}{\rho_S\alpha\omega h R_{\min}}\int_0^t\|\eta\|^2d\tau.
\end{aligned}$$

Proof.

$$\left|\int_0^t\int_{\Omega(t)}\frac{A(t)}{L}v_z d\boldsymbol{x}d\tau\right| \leq \frac{\rho_F\alpha\omega}{2}\int_0^t\|v_z\|_{L^2(\Omega(\tau))}^2d\tau + \frac{1}{2\rho_F\alpha\omega}\int_0^t\frac{|A(\tau)|^2}{L^2}|\Omega(\tau)|d\tau.$$

The size of $\Omega(t)$ can be estimated as $|\Omega(t)| = \pi\int_0^L(R+\eta)^2dz \leq 2\pi\int_0^L(R^2+\eta^2)dz$. Using the assumption of the lemma implies the statement. □

PARAMETERS	*AORTA/ILIACS*
Char. radius $R(m)$	0.003-0.012, [12]
Char. length $L(m)$	0.065-0.2
Dyn. viscosity $\mu(\frac{kg}{ms})$	3.5×10^{-3}
Young's modulus E(Pa)	10^5-10^6 [11]
Wall thickness h(m)	$1-2\times 10^{-3}$ [12]
Wall density $\rho_S(kg/m^3)$	1100, [12]
Fluid density $\rho_F(kg/m^3)$	1050

Table 1: Table with parameter values

The assumption of Lemma 3.3 is fulfilled for our underlying application to blood flow. Namely, as $\|A\|_\infty \leq \|p\|_\infty$ the inequality is satisfied because the left–hand side of inequality $\frac{h}{L}\frac{R_{\min}}{L} \leq \frac{\rho_F}{\rho_S}$ is of order ε and the right–hand side of order one, see Table 1.

Now we define $y(t)$ as the left–hand side of (3.2)

$$y(t)=\int_0^t\left(\frac{\varrho_F\omega}{2}\|\boldsymbol{v}\|^2_{L^2(\Omega(t))}+2\mu\|D(\boldsymbol{v})\|^2_{L^2(\Omega)}+\pi\omega^3\rho_S hR_{\min}\|\partial_t\eta\|^2+\pi\omega Q_{\min}\|\eta\|^2\right)d\tau$$

and estimate it using Lemma 3.2 and Lemma 3.3 to obtain

$$\begin{aligned}y'(t) \;\leq\; & \left(\alpha+\frac{\|\hat p\|^2_\infty}{\alpha\rho_S\omega^2hR_{\min}Q_{\min}}\right)y(t)+\frac{\pi\omega Q_{\min}}{4}\sup_t\|\eta\|^2+\frac{8\pi R^2_{\max}\omega}{Q_{\min}}\int_0^L\hat p^2dz\\ &+\frac{8\pi\omega LR^2_{\max}}{Q_{\min}}\left(\sup_z\int_0^t|\partial_t\hat p|d\tau\right)^2+\frac{\pi R^2_{\max}}{\rho_F\alpha\omega L}\int_0^t|A(\tau)|^2d\tau.\end{aligned}$$

Now we choose α so that

$$\frac{\|\hat p\|^2_\infty}{\alpha\rho_s\omega^2hR_{\min}Q_{\min}}\leq\alpha$$

and t_0 such that $y'(t_0)=\max_{t\in[0,T]}y'(t)$. Then $y(t)\leq Ty'(t_0)$, for $t\in[0,T]$ and one has the estimate

$$\begin{aligned}y'(t_0) \;\leq\; & 2\alpha Ty'(t_0)+\frac{\pi\omega Q_{\min}}{4}\sup_t\|\eta\|^2+\frac{8\pi R^2_{\max}\omega}{Q_{\min}}\int_0^L\hat p^2dz\\ &+\frac{8\pi\omega LR^2_{\max}}{Q_{\min}}\left(\sup_z\int_0^T|\partial_t\hat p|d\tau\right)^2+\frac{\pi R^2_{\max}}{\rho_F\alpha\omega L}\int_0^T|A(\tau)|^2d\tau.\end{aligned}$$

Now take $\alpha=\frac{1}{4T}$ and obtain the following estimate

$$y'(t)\quad\leq\frac{16\pi LR^2_{\max}\omega}{Q_{\min}}\left(\sup_{z,t}|\hat p|^2+\left(\sup_z\int_0^t\hat p_t d\tau\right)^2\right)+\frac{8T\pi R^2_{\max}}{\rho_F\omega L}\int_0^t|A(\tau)|^2d\tau.$$

Now we choose the characteristic frequency ω so that all terms on the right–hand side contribute with the same weight. We set the coefficients in the estimate to be equal and obtain

$$\omega = \frac{1}{L}\sqrt{\frac{Q_{\min}}{2\rho_F}}; \tag{3.3}$$

then ωL, in the constant cross–section case ($R = R_{\max}$), is exactly the same as the structure "sound speed" obtained by Fung [7].

Theorem 3.1 *The solution $(\boldsymbol{v}, \eta)$ of the fluid-structure problem satisfies the estimate*

$$\frac{\varrho_F}{2}\|\boldsymbol{v}\|^2_{L^2(\Omega(t))} + 2\mu\|D(\boldsymbol{v})\|^2_{L^2(\Omega)} + \pi\omega^2\rho_S h R_{\min}\left\|\frac{\partial\eta}{\partial t}\right\|^2 + \frac{\pi}{2}Q_{\min}\|\eta\|^2 \;\leq\; \frac{16\pi L R^2_{\max}}{Q_{\min}}\,\mathcal{P}^2,$$

where $\mathcal{P}^2 := \sup_{z,t}|\hat{p}|^2 + \left(\sup_z \int_0^t |\partial_t\hat{p}|d\tau\right)^2 + T\int_0^t |A(\tau)|^2$.

Corollary 3.1 *The solution $(\boldsymbol{v}, \eta)$ of the fluid-structure problem satisfies the estimates*

$$\frac{1}{R^2_{\max}\pi L}\|\boldsymbol{v}\|^2 \leq \frac{32}{\varrho_F Q_{\min}}\mathcal{P}^2, \qquad \frac{1}{L}\|\eta\|^2 \leq \frac{32R^2_{\max}}{Q^2_{\min}}\mathcal{P}^2.$$

4 The reduced problem

4.1 Nondimensional equations

Since the a priori estimates obtained from Theorem 3.1 present the upper bounds for the behavior of the unknown functions we use the scaled upper bounds to only capture how the magnitude of the unknown functions changes with a given parameter. Using these estimates we will be able to derive the nondimensional problem and to detect the small terms. We introduce the nondimensional variables (beside $\overline{t} = \omega t$ which was introduced previously)

$$\overline{r} = r/R_{\max}, \quad \overline{z} = z/L$$

and the nondimensional functions $\overline{R}, \overline{Q}, \overline{\boldsymbol{v}}, \overline{\eta}, \overline{p}$ by

$$\begin{aligned}
R(L\overline{z}) &= R_{\max}\overline{R}(\overline{z}),\\
Q(L\overline{z}) &= Q_{\min}\overline{Q}(\overline{z}),\\
\boldsymbol{v}(R_{\max}\overline{r}, L\overline{z}, \overline{t}) &= V\overline{\boldsymbol{v}}(\overline{r}, \overline{z}, \overline{t}), \qquad V = \sqrt{\frac{1}{2\varrho_F Q_{\min}}}\mathcal{P},\\
\eta(L\overline{z}, \overline{t}) &= \Xi\overline{\eta}(\overline{z}, \overline{t}), \qquad \Xi = \frac{R_{\max}}{Q_{\min}}\mathcal{P},\\
p(R_{\max}\overline{r}, L\overline{z}, \overline{t}) &= \varrho_F V^2\overline{p}(\overline{r}, \overline{z}, \overline{t})
\end{aligned}$$

and denote

$$\varepsilon = \frac{R_{\max}}{L}, \qquad \delta = \frac{\Xi}{R_{\max}}, \qquad \gamma = \frac{h}{R_{\max}}.$$

The nondimensional equations are then given by:

a) the Navier–Stokes equations

$$\begin{aligned}
&\mathrm{Sh}\frac{\partial \overline{v}_r}{\partial \overline{t}} + \frac{1}{\varepsilon}\overline{v}_r\frac{\partial \overline{v}_r}{\partial \overline{r}} + \overline{v}_z\frac{\partial \overline{v}_r}{\partial \overline{z}} - \frac{1}{\mathrm{Re}}\left(\frac{\partial}{\partial \overline{r}}\left(\frac{1}{\overline{r}}\frac{\partial}{\partial \overline{r}}\left(\overline{r}\overline{v}_r\right)\right) + \varepsilon^2\frac{\partial^2 \overline{v}_r}{\partial \overline{z}^2}\right) + \frac{1}{\varepsilon}\frac{\partial \overline{p}}{\partial \overline{r}} = 0,\\
&\mathrm{Sh}\frac{\partial \overline{v}_z}{\partial \overline{t}} + \frac{1}{\varepsilon}\overline{v}_r\frac{\partial \overline{v}_z}{\partial \overline{r}} + \overline{v}_z\frac{\partial \overline{v}_z}{\partial \overline{z}} - \frac{1}{\mathrm{Re}}\left(\frac{1}{\overline{r}}\frac{\partial}{\partial \overline{r}}\left(\overline{r}\frac{\partial \overline{v}_z}{\partial \overline{r}}\right) + \varepsilon^2\frac{\partial^2 \overline{v}_z}{\partial \overline{z}^2}\right) + \frac{\partial \overline{p}}{\partial \overline{z}} = 0, \qquad (4.1)\\
&\frac{1}{\varepsilon}\frac{1}{\overline{r}}\frac{\partial}{\partial \overline{r}}\left(\overline{r}\overline{v}_r\right) + \frac{\partial \overline{v}_z}{\partial \overline{z}} = 0,
\end{aligned}$$

where $\mathrm{Sh} = \frac{\omega L}{V}$ and $\mathrm{Re} = \frac{\rho_F V R_{\max}^2}{\mu L}$ are the Strouhal and the Reynolds numbers. Note that the nondimensional parameters Sh and Re which are typically used to determine the flow regimes, are given, as a consequence of our a priori estimates, in terms of the parameters in the problem, such as the Young's modulus, the Poisson ratio, etc. They incorporate the information about both the fluid part of the problem (given via V and μ) and the behavior of the membrane (given via E, ω and σ).

b) the linear membrane shell equations:

$$\begin{aligned}
&\int_0^1 \frac{\rho_S}{2\rho_F}\mathcal{P}\gamma\varepsilon^2\frac{\partial^2 \overline{\eta}}{\partial \overline{t}^2}\xi\overline{R}\sqrt{1+\varepsilon^2\left(\overline{R}'\right)^2}d\overline{z}\\
&+\int_0^1 \frac{\sigma E}{1-\sigma^2}\gamma\delta\left(\frac{\varepsilon^2\overline{R}'}{1+\varepsilon^2\left(\overline{R}'\right)^2}\overline{\eta}' + \frac{1}{\overline{R}}\overline{\eta}\right)\left(\frac{\varepsilon^2\overline{R}'}{1+\varepsilon^2\left(\overline{R}'\right)^2}\xi' + \frac{1}{\overline{R}}\xi\right)\overline{R}\sqrt{1+\varepsilon^2\left(\overline{R}'\right)^2}d\overline{z}\\
&+\int_0^1 \frac{E}{1+\sigma}\gamma\delta\left(\left(\frac{\varepsilon\overline{R}'}{1+\varepsilon^2\left(\overline{R}'\right)^2}\right)^2\varepsilon^2\overline{\eta}'\xi' + \frac{1}{\overline{R}^2}\overline{\eta}\xi\right)\overline{R}\sqrt{1+\varepsilon^2\left(\overline{R}'\right)^2}d\overline{z} \qquad (4.2)\\
&+\int_0^1 \gamma\delta T^0_{\theta\theta}\frac{\overline{\eta}\xi}{\overline{R}^2}\overline{R}\sqrt{1+\varepsilon^2\left(\overline{R}'\right)^2}d\overline{z} = \int_0^1 f_r\xi\overline{R}\sqrt{1+\varepsilon^2\left(\overline{R}'\right)^2}d\overline{z}, \qquad \xi\in H^1_0(0,1);
\end{aligned}$$

c) the kinematic contact condition

$$\frac{1}{\varepsilon}\overline{v}_r(\overline{R}+\delta\overline{\eta}(z,t),\overline{z},\overline{t}) = \frac{\partial\overline{\eta}(\overline{z},\overline{t})}{\partial\overline{t}}, \quad \overline{v}_z(\overline{R}+\delta\overline{\eta}(\overline{z},\overline{t}),\overline{z},\overline{t}) = 0;$$

d) the dynamic contact condition

$$f_r = \rho_F V^2\left((\overline{p}-\overline{p}_{\mathrm{ref}}) + \frac{1}{\mathrm{Re}}\left(\left(\varepsilon\overline{R}'+\varepsilon\delta\overline{\eta}'\right)\left(\varepsilon^2\frac{\partial\overline{v}_r}{\partial\overline{z}} + \varepsilon\frac{\partial\overline{v}_z}{\partial\overline{r}}\right) - 2\varepsilon\frac{\partial\overline{v}_r}{\partial\overline{r}}\right)\right)\frac{1+\delta\frac{\overline{\eta}}{\overline{R}}}{\sqrt{1+\varepsilon^2\left(\overline{R}'\right)^2}}.$$

4.2 The ε reduction

Now we construct the ε^2 approximation of the starting problem in Section 2. First note that due to the incompressibility equation one has that $\overline{v}_r/\varepsilon = O(1)$ (this was noted in the a priori estimates as they were derived for the vector $\boldsymbol{v}$). Then we build an ε^2–approximation by taking only the two leading ε approximations in each of the equations a)–d) from Section 4.1. Here we implicitly assume that $\overline{R}' \approx 1$ (equivalently $R' \approx \varepsilon$) which sets a restriction on the geometry of the problem. We obtain

a) the hydrostatic approximation of equations (4.1)

$$\begin{aligned}
&\frac{\partial \overline{p}}{\partial \overline{r}} = 0,\\
&\mathrm{Sh}\frac{\partial \overline{v}_z}{\partial \overline{t}} + \frac{1}{\varepsilon}\overline{v}_r\frac{\partial \overline{v}_z}{\partial \overline{r}} + \overline{v}_z\frac{\partial \overline{v}_z}{\partial \overline{z}} - \frac{1}{\mathrm{Re}}\left(\frac{1}{\overline{r}}\frac{\partial}{\partial \overline{r}}\left(\overline{r}\frac{\partial \overline{v}_z}{\partial \overline{r}}\right)\right) + \frac{\partial \overline{p}}{\partial \overline{z}} = 0,\\
&\frac{1}{\varepsilon}\frac{1}{\overline{r}}\frac{\partial}{\partial \overline{r}}\left(\overline{r}\overline{v}_r\right) + \frac{\partial \overline{v}_z}{\partial \overline{z}} = 0.
\end{aligned} \tag{4.3}$$

b) the linear membrane shell approximation of equation (4.2)

$$\int_0^1 \left(\frac{E}{1-\sigma^2} + T^0_{\theta\theta}\right)\gamma\delta\frac{1}{\overline{R}}\overline{\eta}\xi d\overline{z} = \int_0^1 f_r\xi\overline{R}d\overline{z}, \qquad \xi \in H^1_0(0,1);$$

c) the kinematic contact condition

$$\frac{1}{\varepsilon}\overline{v}_r(\overline{R}+\delta\overline{\eta}(z,t),\overline{z},\overline{t}) = \frac{\partial\overline{\eta}(\overline{z},\overline{t})}{\partial\overline{t}}, \quad \overline{v}_z(\overline{R}+\delta\overline{\eta}(\overline{z},\overline{t}),\overline{z},\overline{t}) = 0;$$

d) the dynamic contact condition

$$f_r = \rho_F V^2\left(\overline{p}-\overline{p}_{\mathrm{ref}}\right)\left(1+\delta\frac{\overline{\eta}}{\overline{R}}\right).$$

Note that the force–displacement relationship in the reduced shell model is algebraic. Together with the hydrostatic approximation of the flow and the dynamic contact condition at the interface this implies the algebraic pressure–displacement relationship called the Laplace law

$$\overline{p}-\overline{p}_{\mathrm{ref}} = \frac{\gamma\delta}{\rho_F V^2}\left(\frac{E}{1-\sigma^2}+T^0_{\theta\theta}\right)\frac{1}{\overline{R}}\frac{\overline{\eta}}{\overline{R}+\delta\overline{\eta}}.$$

In the asymptotic reduction of the equations we have lost the boundary conditions for the membrane shell. This leads to the boundary layer near the boundary to accommodate the transition from the zero displacement to the displacement dictated by the dynamic pressure condition. In [4] it was proved that the contamination of the flow by the boundary layer decays exponentially fast away from the inlet/outlet boundaries. Therefore, except for a small neighborhood of the inlet/outlet boundary, the displacement will follow the dynamics determined by the time-dependent dynamic pressure.

Furthermore, notice that the ε^2-approximation of the inlet and outlet boundary conditions consists of prescribing only the pressure and not the dynamic pressure.

The system a)–d), together with the boundary and initial conditions from e), f) in Section 2, is a closed free-boundary problem. It is a simplification of the problem from Section 2 but still difficult to study from numerical and theoretical viewpoint. Therefore, we perform further reductions.

4.3 The ε expansion

To derive the reduced effective equations that approximate the original three-dimensional problem to the ε^2 accuracy we rely on the ideas presented by the authors in [5] utilizing homogenization theory in porous media flows. Once the proper motivation is established the calculation of the effective equations itself can be performed using formal asymptotic theory, which we now utilize.

The physiological flow conditions are such that we can rescale the Strouhal and the Reynolds number

$$\mathrm{Sh}_0 = \varepsilon \mathrm{Sh}, \qquad \mathrm{Re}_0 = \mathrm{Re}/\varepsilon$$

to obtain the numbers of usual magnitude for a laminar flow. It implies that the axial momentum equation (the second equation in (4.3)) can be written as

$$\mathrm{Sh}_0 \frac{\partial \overline{v}_z}{\partial \overline{t}} + \overline{v}_r \frac{\partial \overline{v}_z}{\partial \overline{r}} + \varepsilon \overline{v}_z \frac{\partial \overline{v}_z}{\partial \overline{z}} - \frac{1}{\mathrm{Re}_0}\left(\frac{1}{\overline{r}}\frac{\partial}{\partial \overline{r}}\left(\overline{r}\frac{\partial \overline{v}_z}{\partial \overline{r}}\right)\right) + \frac{\partial \overline{\overline{p}}}{\partial \overline{z}} = 0, \tag{4.4}$$

where $\overline{\overline{p}} = \frac{R_{\max}}{L\rho_F V^2} p$. Now we assume the following expansions with respect to ε

$$\overline{v}_z = \overline{v}_z^0 + \varepsilon \overline{v}_z^1 + \cdots, \qquad \overline{v}_r = \varepsilon \overline{v}_r^1 + \cdots, \qquad \overline{\overline{p}} = \overline{\overline{p}}^0 + \varepsilon \overline{\overline{p}}^1 + \cdots, \qquad \overline{\eta} = \overline{\eta}^0 + \varepsilon \overline{\eta}^1 + \cdots$$

and plug them into a)–d) but with the equation (4.3) replaced by (4.4). Then we obtain

The 0th order terms

$$\begin{aligned}
&\mathrm{Sh}_0 \frac{\partial \overline{v}_z^0}{\partial \overline{t}} - \frac{1}{\mathrm{Re}_0}\left(\frac{1}{\overline{r}}\frac{\partial}{\partial \overline{r}}\left(\overline{r}\frac{\partial \overline{v}_z^0}{\partial \overline{r}}\right)\right) + \frac{\partial \overline{\overline{p}}^0}{\partial \overline{z}} = 0,\\
&\frac{1}{\overline{r}}\frac{\partial}{\partial \overline{r}}\left(\overline{r}\overline{v}_r^1\right) + \frac{\partial \overline{v}_z^0}{\partial \overline{z}} = 0,\\
&\overline{v}_r^1(\overline{R} + \delta\overline{\eta}^0(z,t), \overline{z}, \overline{t}) = \frac{\partial \overline{\eta}^0(\overline{z}, \overline{t})}{\partial \overline{t}}, \quad \overline{v}_z^0(\overline{R} + \delta\overline{\eta}^0(\overline{z}, \overline{t}), \overline{z}, \overline{t}) = 0,\\
&\overline{\overline{p}}^0 - \overline{\overline{p}}_{\mathrm{ref}} = \frac{R_{\max}\gamma\delta}{\rho_F V^2 L}\left(\frac{E}{1-\sigma^2} + T_{\theta\theta}^0\right)\frac{1}{\overline{\overline{R}}}\frac{\overline{\eta}^0}{\overline{R} + \delta\overline{\eta}^0},
\end{aligned}$$

The 1st order terms

$$\mathrm{Sh}_0 \frac{\partial \overline{v}_z^1}{\partial \overline{t}} + \overline{v}_r^1 \frac{\partial \overline{v}_z^0}{\partial \overline{r}} + \overline{v}_z^0 \frac{\partial \overline{v}_z^0}{\partial \overline{z}} - \frac{1}{\mathrm{Re}_0}\left(\frac{1}{\overline{r}}\frac{\partial}{\partial \overline{r}}\left(\overline{r}\frac{\partial \overline{v}_z^1}{\partial \overline{r}}\right)\right) + \frac{\partial \overline{\overline{p}}^1}{\partial \overline{z}} = 0,$$

$$
\begin{aligned}
&\frac{1}{\overline{r}}\frac{\partial}{\partial\overline{r}}\left(\overline{r}\overline{v}_r^2\right)+\frac{\partial\overline{v}_z^1}{\partial\overline{z}}=0,\\
&\overline{v}_r^2(\overline{R}+\delta\overline{\eta}^0(z,t),\overline{z},\overline{t})+\frac{\partial\overline{v}_r^1}{\partial\overline{r}}(\overline{R}+\delta\overline{\eta}^0(z,t),\overline{z},\overline{t})\delta\overline{\eta}^1(\overline{z},\overline{t})=\frac{\partial\overline{\eta}^1(\overline{z},\overline{t})}{\partial\overline{t}},\\
&\overline{v}_z^1(\overline{R}+\delta\overline{\eta}^0(\overline{z},\overline{t}),\overline{z},\overline{t})+\frac{\partial\overline{v}_z^1}{\partial\overline{r}}(\overline{R}+\delta\overline{\eta}^0(\overline{z},\overline{t}),\overline{z},\overline{t})\delta\overline{\eta}^1(\overline{z},\overline{t})=0,\\
&\overline{\overline{p}}^1=\frac{R_{\max}\gamma\delta}{\rho_F V^2 L}\left(\frac{E}{1-\sigma^2}+T^0_{\theta\theta}\right)\frac{\overline{\eta}^1}{(\overline{R}+\delta\overline{\eta}^0)^2}.
\end{aligned}
$$

Now we assume that the displacement of the structure is small compared to the radius: $\delta\le\varepsilon$. Therefore the model without $\overline{\overline{p}}^1$ and $\overline{\eta}^1$ (and of course $\overline{v}_r^2$) is an ε^2 approximation as well. Then integrating the incompressibility condition over the cross–section in the 0th order terms equation and using the kinematic contact condition we obtain the following

The 0th order approximation

$$
\begin{aligned}
&\frac{\partial}{\partial\overline{t}}(\overline{R}+\delta\overline{\eta}^0)^2+2\delta\frac{\partial}{\partial\overline{z}}\int_0^{\overline{R}+\delta\overline{\eta}^0}\overline{r}\overline{v}_z^0 d\overline{r}=0,\\
&\mathrm{Sh}_0\frac{\partial\overline{v}_z^0}{\partial\overline{t}}-\frac{1}{\mathrm{Re}_0}\left(\frac{1}{\overline{r}}\frac{\partial}{\partial\overline{r}}\left(\overline{r}\frac{\partial\overline{v}_z^0}{\partial\overline{r}}\right)\right)=-\frac{\partial\overline{\overline{p}}^0}{\partial\overline{z}},\\
&\overline{\overline{p}}^0-\overline{\overline{p}}_{\mathrm{ref}}=\frac{R_{\max}\gamma\delta}{\rho_F V^2 L}\left(\frac{E}{1-\sigma^2}+T^0_{\theta\theta}\right)\frac{1}{\overline{\overline{R}}}\frac{\overline{\eta}^0}{\overline{R}+\delta\overline{\eta}^0},
\end{aligned}
$$

with the initial and boundary conditions

$$
\begin{aligned}
&\overline{v}_z^0|_{\overline{r}=0}-\ \text{bounded},\quad \overline{v}_z^0|_{\overline{r}=\overline{R}+\delta\overline{\eta}^0}=0,\quad \overline{v}_z^0|_{\overline{t}=0}=0,\\
&\overline{\eta}^0|_{\overline{t}=0}=0,\quad \overline{\overline{p}}^0|_{\overline{z}=0}=\overline{\overline{p}}_{\mathrm{ref}}+\frac{R_{\max}}{\rho_F V^2 L}P_0,\quad \overline{\overline{p}}^0|_{\overline{z}=1}=\overline{\overline{p}}_{\mathrm{ref}}+\frac{R_{\max}}{\rho_F V^2 L}P_L.
\end{aligned}
$$

The 1st order corrector

$$
\begin{aligned}
&\frac{\partial}{\partial\overline{r}}(\overline{r}\overline{v}_r^1)+\frac{\partial}{\partial\overline{z}}(\overline{r}\overline{v}_z^0)=0,\\
&\mathrm{Sh}_0\frac{\partial\overline{v}_z^1}{\partial\overline{t}}-\frac{1}{\mathrm{Re}_0}\frac{1}{\overline{r}}\frac{\partial}{\partial\overline{r}}\left(\overline{r}\frac{\partial\overline{v}_z^1}{\partial\overline{r}}\right)=-\overline{v}_r^1\frac{\partial\overline{v}_z^0}{\partial\overline{r}}-\overline{v}_z^0\frac{\partial\overline{v}_z^0}{\partial\overline{z}},
\end{aligned}
$$

with the initial and boundary conditions

$$
\begin{aligned}
&\overline{v}_r^1|_{\overline{r}=0}-\ \text{bounded},\qquad \overline{v}_r^1|_{\overline{r}=\overline{R}+\delta\overline{\eta}^0}=\frac{\partial\overline{\eta}^0}{\partial\overline{t}},\\
&\overline{v}_z^1|_{\overline{r}=0}-\ \text{bounded},\qquad \overline{v}_z^1|_{\overline{r}=\overline{R}+\delta\overline{\eta}^0}=0,\qquad \overline{v}_z^1|_{\overline{t}=0}=0.
\end{aligned}
$$

4.4 The δ expansion

The 0th order approximation together with the 1st order corrector make a closed reduced model, but still with the lateral boundary which is a free boundary. Therefore we make

a further simplification by using the assumption $\delta \leq \varepsilon$ and by expanding the problem with respect to δ:

$$\overline{v}_z^0 = \overline{v}_z^{0,0} + \delta \overline{v}_z^{0,1} + \cdots, \quad \overline{p} = \overline{p}^{0,0} + \delta \overline{p}^{0,1} + \cdots, \quad \overline{\eta}^0 = \overline{\eta}^{0,0} + \delta \overline{\eta}^{0,1} + \cdots.$$

We obtain the $0,0$–order approximation

$$\begin{aligned}
&\frac{\partial \overline{\eta}^{0,0}}{\partial \overline{t}} + \frac{1}{\overline{\overline{R}}} \frac{\partial}{\partial \overline{z}} \int_0^{\overline{R}} \overline{r} \overline{v}_z^{0,0} d\overline{r} = 0, \\
&\mathrm{Sh}_0 \frac{\partial \overline{v}_z^{0,0}}{\partial \overline{t}} - \frac{1}{\mathrm{Re}_0} \frac{1}{\overline{r}} \frac{\partial}{\partial \overline{r}} \left(\overline{r} \frac{\partial \overline{v}_z^{0,0}}{\partial \overline{r}} \right) = - \frac{\partial \overline{\overline{p}}^{0,0}}{\partial \overline{z}}, \\
&\overline{\overline{p}}^{0,0} = \overline{\overline{p}}_{\mathrm{ref}} + \frac{R_{\max} \gamma \delta}{\rho_F V^2 L} \left(\frac{E}{1-\sigma^2} + T^0_{\theta\theta} \right) \frac{\overline{\eta}^{0,0}}{\overline{R}^2},
\end{aligned}$$

and the $0,0$–order boundary and initial conditions

$$\begin{aligned}
&\overline{v}_z^{0,0}|_{\overline{r}=0} - \text{ bounded}, \quad \overline{v}_z^{0,0}|_{\overline{r}=\overline{R}} = 0, \quad \overline{v}_z^{0,0}|_{\overline{t}=0} = 0, \\
&\overline{\eta}^{0,0}|_{\overline{t}=0} = 0, \quad \overline{\overline{p}}^{0,0}|_{\overline{z}=0} = \overline{\overline{p}}_{\mathrm{ref}} + \frac{R_{\max}}{\rho_F V^2 L} P_0, \quad \overline{\overline{p}}^{0,0}|_{\overline{z}=1} = \overline{\overline{p}}_{\mathrm{ref}} + \frac{R_{\max}}{\rho_F V^2 L} P_L.
\end{aligned}$$

The δ corrector is given by

$$\begin{aligned}
&\frac{\partial}{\partial \overline{t}} \overline{\eta}^{0,1} + \frac{1}{\overline{\overline{R}}} \frac{\partial}{\partial \overline{z}} \int_0^{\overline{R}} \overline{r} \overline{v}_z^{0,1} d\overline{r} = - \frac{1}{2\overline{R}} \frac{\partial}{\partial \overline{t}} \left(\overline{\eta}^{0,0} \right)^2, \\
&\mathrm{Sh}_0 \frac{\partial \overline{v}_z^{0,1}}{\partial \overline{t}} - \frac{1}{\mathrm{Re}_0} \frac{1}{\overline{r}} \frac{\partial}{\partial \overline{r}} \left(\overline{r} \frac{\partial \overline{v}_z^{0,1}}{\partial \overline{r}} \right) = - \frac{\partial \overline{\overline{p}}^{0,1}}{\partial \overline{z}}, \\
&\overline{\overline{p}}^{0,1} = \frac{R_{\max} \gamma \delta}{\rho_F V^2 L} \left(\frac{E}{1-\sigma^2} + T^0_{\theta\theta} \right) \frac{1}{\overline{\overline{R}}} \left(\frac{\overline{\eta}^{0,1}}{\overline{R}} - \frac{(\overline{\eta}^{0,0})^2}{\overline{R}^2} \right),
\end{aligned}$$

with the boundary and initial conditions

$$\begin{aligned}
&\overline{v}_z^{0,1}|_{\overline{r}=0} - \text{ bounded}, \quad \overline{v}_z^{0,1}|_{\overline{r}=\overline{R}} = - \overline{\eta}^{0,0} \frac{\partial \overline{v}_z^{0,0}}{\partial \overline{r}}|_{\overline{r}=\overline{R}}, \quad \overline{v}_z^{0,1}|_{\overline{t}=0} = 0, \\
&\overline{\eta}^{0,1}|_{\overline{t}=0} = 0, \quad \overline{\eta}^{0,1}|_{\overline{z}=0} = 0, \quad \overline{\eta}^{0,1}|_{\overline{z}=1} = 0.
\end{aligned}$$

The δ expansion in the ε correction is just a linearization of the free-boundary problem since its correctors contain only the ε^2 terms. So the the equations of the $1,0$ approximation are

$$\begin{aligned}
&\frac{\partial}{\partial \overline{r}} (\overline{r} \overline{v}_r^{1,0}) + \frac{\partial}{\partial \overline{z}} (\overline{r} \overline{v}_z^{0,0}) = 0, \\
&\mathrm{Sh}_0 \frac{\partial \overline{v}_z^{1,0}}{\partial \overline{t}} - \frac{1}{\mathrm{Re}_0} \frac{1}{\overline{r}} \frac{\partial}{\partial \overline{r}} \left(\overline{r} \frac{\partial \overline{v}_z^{1,0}}{\partial \overline{r}} \right) = - \overline{v}_r^{1,0} \frac{\partial \overline{v}_z^{0,0}}{\partial \overline{r}} - \overline{v}_z^{0,0} \frac{\partial \overline{v}_z^{0,0}}{\partial \overline{z}},
\end{aligned}$$

with the initial and boundary conditions

$$\begin{aligned}
&\overline{v}_r^{1,0}|_{\overline{r}=0} - \text{ bounded}, \qquad \overline{v}_r^{1,0}|_{\overline{r}=\overline{R}} = \frac{\partial \overline{\eta}^{0,0}}{\partial \overline{t}}, \\
&\overline{v}_z^{1,0}|_{\overline{r}=0} - \text{ bounded}, \qquad \overline{v}_z^{1,0}|_{\overline{r}=\overline{R}} = 0, \qquad \overline{v}_z^{1,0}|_{\overline{t}=0} = 0.
\end{aligned}$$

4.5 The reduced model in dimensional form

The nondimensional form of the equations allowed us to detect smaller terms. Now we have to go back to the physical domain and to write down the model in terms of the physical quantities

$$v_z = v_z^{0,0} + v_z^{0,1} + v_z^{1,0}, \qquad v_r = v_r^{1,0}, \quad \eta = \eta^{0,0} + \eta^{0,1} + \eta^{1,0}, \quad p = p^{0,0} + p^{0,1},$$

where

$$\begin{aligned}
&v_z^{0,0} = V\overline{v}_z^{0,0}, \quad v_z^{0,1} = \delta V\overline{v}_z^{0,1}, \quad v_z^{1,0} = \varepsilon V\overline{v}_z^{1,0}, \quad v_r^{1,0} = \varepsilon V\overline{v}_r^{1,0},\\
&\eta^{0,0} = \Xi\overline{\eta}^{0,0}, \quad \eta^{0,1} = \delta\Xi\overline{\eta}^{0,1}, \quad p^{0,0} = \rho_F V^2\frac{L}{R_{\max}}\overline{\overline{p}}^{0,0}, \quad p^{0,1} = \rho_F V^2\frac{L}{R_{\max}}\delta\overline{\overline{p}}^{0,1}.
\end{aligned}$$

The 0th order model is given by

$$\begin{aligned}
&\frac{\partial\eta^{0,0}}{\partial t} + \frac{1}{R}\frac{\partial}{\partial z}\int_0^R r v_z^{0,0}dr = 0,\\
&\varrho_F\frac{\partial v_z^{0,0}}{\partial t} - \mu\frac{1}{r}\frac{\partial}{\partial r}\left(r\frac{\partial v_z^{0,0}}{\partial r}\right) = -\frac{\partial}{\partial z}\left(\left(\frac{E}{1-\nu^2} + T_{\theta\theta}^0\right)\frac{h}{R^2}\eta^{0,0}\right),\\
&v_z^{0,0}|_{r=0} - \text{ bounded}, \quad v_z^{0,0}|_{t=R} = 0, \quad v_z^{0,0}|_{t=0} = 0,\\
&\eta^{0,0}|_{t=0} = 0, \quad \eta^{0,0}|_{z=0} = P_0/C, \quad \eta^{0,0}|_{z=L} = P_L/C.
\end{aligned} \tag{4.5}$$

The δ correction

$$\begin{aligned}
&\frac{\partial\eta^{0,1}}{\partial t} + \frac{1}{R}\frac{\partial}{\partial z}\int_0^R r v_z^{0,1}dr = -\frac{1}{2R}\frac{\partial}{\partial t}\left(\eta^{0,0}\right)^2,\\
&\varrho_F\frac{\partial v_z^{0,1}}{\partial t} - \mu\frac{1}{r}\frac{\partial}{\partial r}\left(r\frac{\partial v_z^{0,1}}{\partial r}\right) = -\frac{\partial}{\partial z}\left(\left(\frac{E}{1-\nu^2} + T_{\theta\theta}^0\right)\frac{h}{R^2}\left(\eta^{0,1} - \frac{(\eta^{0,0})^2}{R}\right)\right)\\
&v_z^{0,1}|_{r=0} - \text{ bounded}, \quad v_z^{0,1}|_{r=R} = -\eta^{0,0}\frac{\partial v_z^{0,0}}{\partial r}|_{r=R}, \quad v_z^{0,1}|_{t=0} = 0,\\
&\eta^{0,1}|_{t=0} = 0, \quad \eta^{0,1}|_{z=0} = 0, \quad \eta^{0,1}|_{z=L} = 0.
\end{aligned} \tag{4.6}$$

The ε correction

$$v_r^{1,0}(r,z,t) = \frac{1}{r}\left(R\frac{\partial\eta^{0,0}}{\partial t} + \int_r^R \xi\frac{\partial v_z^{0,0}}{\partial z}(\xi,z,t)d\xi\right), \tag{4.7}$$

$$\begin{aligned}
&\rho_F\frac{\partial v_z^{1,0}}{\partial t} - \mu\frac{1}{r}\frac{\partial}{\partial r}\left(r\frac{\partial v_z^{1,0}}{\partial r}\right) = -\rho_F\left(v_r^{1,0}\frac{\partial v_z^{0,0}}{\partial r} + v_z^{0,0}\frac{\partial v_z^{0,0}}{\partial z}\right),\\
&v_z^{1,0}|_{\overline{r}=0} - \text{ bounded}, \qquad v_z^{1,0}|_{r=R} = 0, \qquad v_z^{1,0}|_{t=0} = 0.
\end{aligned} \tag{4.8}$$

In [5] it was observed that (4.5) can be solved by considering the auxiliary problem

$$\begin{aligned}
&\frac{\partial\zeta}{\partial t} - \frac{1}{r}\frac{\partial}{\partial r}\left(r\frac{\partial\zeta}{\partial r}\right) = 0 \quad \text{ in } \ (0,R)\times(0,\infty)\\
&\zeta|_{r=0} \ \text{ is bounded }, \quad \zeta|_{R=0} = 0 \ \text{ and } \ \zeta|_{t=0} = 1,
\end{aligned}$$

and the mean of ζ in the radial direction $\mathcal{K}(t) = 2\int_0^R \zeta(r,t)\, rdr$, which can both be evaluated in terms of the Bessel's functions. Our solution can then be written in terms of the following operator $(\mathcal{K} \star f)(z,t) := \int_0^t \mathcal{K}(\frac{\mu(t-\tau)}{\rho_F}) f(z,\tau) d\tau$. Now the problem for $\eta^{0,0}$ expressed in terms of

$$p^{0,0} = C\eta^{0,0}, \qquad C = \left(\frac{E}{1-\nu^2} + T^0_{\theta\theta}\right)\frac{h}{R^2} \tag{4.9}$$

consists of finding $p^{0,0}$ by solving the following initial-boundary value problem of the Biot type with memory:

$$\begin{array}{l} \dfrac{\partial p^{0,0}}{\partial t}(z,t) = \dfrac{C}{2\rho_F R}\dfrac{\partial^2(\mathcal{K}\star p^{0,0})}{\partial z^2}(z,t) \text{ on } (0,L)\times(0,+\infty) \\ p^{0,0}|_{z=0} = P_0, \quad p^{0,0}|_{z=L} = P_L \quad \text{and} \quad p^{0,0}|_{t=0} = 0. \end{array} \tag{4.10}$$

This approach uncovers the visco-elastic nature of the coupled fluid-structure interaction problem since the resulting equations have the form of a Biot system with memory (see [1] and references therein for details).

5 Numerical Method

In [5] we have described a method for numerically solving equations (4.5)-(4.8), but written in form of (4.10), directly using a combination of a finite difference method for the calculation of the displacement and a finite element method for the calculation of the velocity. In this manuscript we describe a direct numerical procedure for solving (4.5)–(4.8). The approximation $1,0$ is straightforward once the approximations $0,0$ and $0,1$ are obtained.

First rewrite the (4.5) approximation in terms of $v_z^{0,0}$ and $p^{0,0}$. Multiply the first equation in (4.5) by C (see (4.9)) and take the derivative with respect to t and then substitute $\frac{\partial v_z^{0,0}}{\partial t}$ from the second equation to obtain

$$\begin{aligned} \frac{\partial^2 p^{0,0}}{\partial t^2} &= -\frac{C}{R}\int_0^R r\frac{\partial}{\partial z}\frac{\partial v_z^{0,0}}{\partial t}dr = -\frac{C}{\rho_F R}\int_0^R r\frac{\partial}{\partial z}\left(\mu\frac{1}{r}\frac{\partial}{\partial r}\left(r\frac{\partial v_z^{0,0}}{\partial r}\right) - \frac{\partial}{\partial z}\left(p^{0,0}\right)\right)dr \\ &= -\frac{C\mu}{\rho_F}\frac{\partial}{\partial z}\left(\frac{\partial v_z^{0,0}}{\partial r}|_{r=R}\right) + \frac{CR}{2\rho_F}\frac{\partial^2 p^{0,0}}{\partial z^2}. \end{aligned}$$

Therefore instead of (4.5), we solve the hyperbolic-parabolic system

$$\frac{\partial^2 p^{0,0}}{\partial t^2} - \frac{CR}{2\rho_F}\frac{\partial^2 p^{0,0}}{\partial z^2} = -\frac{C\mu}{\rho_F}\frac{\partial}{\partial z}\left(\frac{\partial v_z^{0,0}}{\partial r}|_{r=R}\right), \tag{5.1}$$

$$\rho_F\frac{\partial v_z^{0,0}}{\partial t} - \mu\frac{1}{r}\frac{\partial}{\partial r}\left(r\frac{\partial v_z^{0,0}}{\partial r}\right) = -\frac{\partial p^{0,0}}{\partial z}, \tag{5.2}$$

with the initial and boundary conditions

$$v_z^{0,0}|_{r=0} - \text{ bounded}, \quad v_z^{0,0}|_{t=R} = 0, \quad v_z^{0,0}|_{t=0} = 0,$$
$$p^{0,0}|_{t=0} = 0, \quad p^{0,0}|_{z=0} = P_0, \quad p^{0,0}|_{z=L} = P_L.$$

Perform the same computation for the $0,1$ approximation and replace (4.6) by

$$\frac{\partial^2 p^{0,1}}{\partial t^2} - \frac{CR}{2\rho_F}\frac{\partial^2 p^{0,1}}{\partial z^2} = -\frac{C\mu}{\rho_F}\frac{\partial}{\partial z}\left(\frac{\partial v_z^{0,0}}{\partial r}|_{r=R}\right) - \frac{CR}{2\rho_F}\frac{\partial^2}{\partial z^2}\left(\frac{C}{R}(\eta^{0,0})^2\right) - \frac{C}{2R}\frac{\partial^2}{\partial t^2}\left(\eta^{0,0}\right)^2, \tag{5.3}$$

$$\rho_F\frac{\partial v_z^{0,1}}{\partial t} - \mu\frac{1}{r}\frac{\partial}{\partial r}\left(r\frac{\partial v_z^{0,1}}{\partial r}\right) = -\frac{\partial}{\partial z}\left(p^{0,1} - \frac{C}{R}(\eta^{0,0})^2\right), \tag{5.4}$$

with the initial and boundary conditions given by

$$v_z^{0,1}|_{r=0} - \text{ bounded}, \quad v_z^{0,1}|_{r=R} = -\eta^{0,0}\frac{\partial v_z^{0,0}}{\partial r}|_{r=R}, \quad v_z^{0,1}|_{t=0} = 0,$$
$$p^{0,1}|_{t=0} = 0, \quad p^{0,1}|_{z=0} = 0, \quad p^{0,1}|_{z=L} = 0.$$

The problems for $(p^{0,0}, v_z^{0,0})$ and $(p^{0,1}, v_z^{0,1})$ are of the same form. It is a coupled system of the hyperbolic (for the displacement of the domain wall) and parabolic equation (for the velocity). The velocity equations are given on the cross–sections $r \in (0, R(z))$ of the domain with no explicit dependence on each other with longitudinal variable z as a parameter. The dependence is incorporated through the wave equation for the displacement of the wall.

The approximation $1,0$ is straightforward once the approximations $0,0$ and $0,1$ are obtained. The systems for the $0,0$ and $0,1$ approximations have the same form, with the mass and stiffness matrices equal for both problems, depending only on the variable z through the cross–section $(0, R(z))$. Thus they are generated only once for each cross–section.

The problems $0,0$ and $0,1$ are solved simultaneously using a time-iteration procedure. First solve the parabolic equation for $v_z^{0,0}$ at the time step t_{i+1} by explicitly evaluating the right–hand side at the time-step t_i. Then solve the wave equation for $\eta^{0,0}$ with the evaluation of the right–hand side at the time-step t_{i+1}. Using these results for $v_z^{0,0}$ and $\eta^{0,0}$, computed at t_{i+1}, obtain a correction at t_{i+1} by repeating the process with the updated values of the right–hand sides. An implicit time discretization is used. The numerical algorithm reads:

1. Approximation $0,0$: for $i = 0$ to n_T
   (a) solve (5.2) at t_{i+1} for $v_z^{0,0}$ using 1D FEM with linear elements
   (b) solve (5.1) at t_{i+1} for $p^{0,0}$ using 1D FEM with C^1 elements
   (c) compute $\eta^{0,0}$

2. Approximation $0,1$: for $i = 0$ to n_T
   (a) solve (5.4) at t_{i+1} for $v_z^{0,1}$ using 1D FEM with linear elements
   (b) solve (5.3) at t_{i+1} for $p^{0,1}$ using 1D FEM with C^1 elements
   (c) compute $\eta^{0,1}$

3. Approximation $1,0$
   (a) solve (4.7) for $v_r^{1,0}$ using numerical integration
   (b) solve (4.8) for $v_z^{1,0}$ using 1D FEM with linear elements

4. Compute the total approximation $v_r = v_r^{1,0}, v_z = v_z^{0,0} + v_z^{0,1} + v_z^{1,0}, \eta = \eta^{0,0} + \eta^{0,1}$.

In this algorithm a sequence of 1D problems is solved, so the numerical complexity is that of 1D solvers. However, leading order two-dimensional effects are captured as shown in Figures 5–7.

6 Numerical results

Numerical simulations were performed for the following set of parameters:

$$\begin{aligned} &\rho_F = 1050 kg/m^3, \quad \mu = 0.0035 kg/ms, \quad L = 0.065 m, \\ &h = 0.0018 m, \quad E = 200000 Pa, \quad \nu = 0.5, p_{\text{ref}} = 85 mmHg, \end{aligned} \tag{6.1}$$

corresponding to the iliac arteries. The inlet and outlet pressure data are shown in

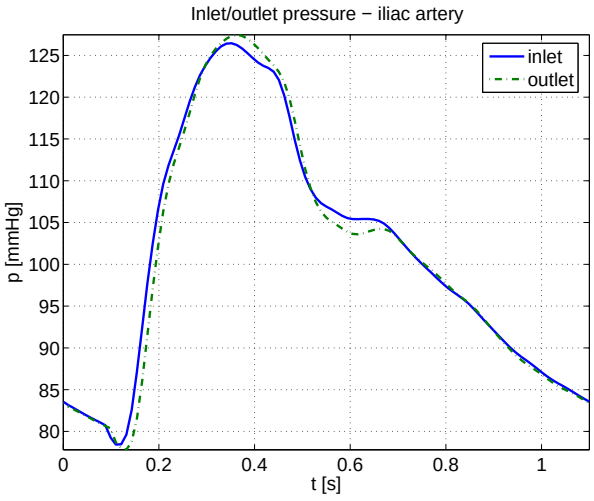

Figure 3: Inlet/outlet pressure

Figure 3. We consider tapered iliac arteries with the radius

$$R(z) = -slope(z - L/2)/L + 0.003, \tag{6.2}$$

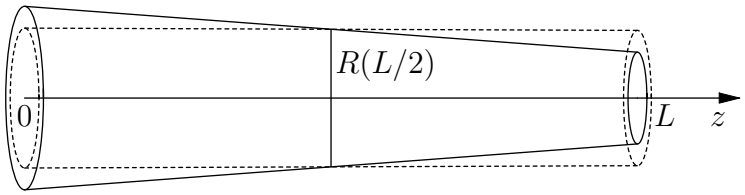

Figure 4: Sketch of the tapered domains

given in meters, where the *slope* takes the value from the set $\{10^{-7}, 10^{-6}, 10^{-5}, 10^{-4}, 2 \cdot 10^{-4}\}$. The mean radius in all examples is $0.003m$. The slope $2 \cdot 10^{-4}$ is typical for the iliac arteries.

A calculation of the non-dimensional parameter values shows that our model can be used to simulate the flow with parameter value given in (6.1). More precisely, for the pressure data shown in Figure 3, the value of the norm $\mathcal{P}$ is around 15000, the average magnitude of the velocity V is $1.15m/s$, the time scale parameter $\omega = 95s^{-1}$, and the Strouhal and Reynolds numbers are

$$Sh = 5.36, \quad Re = 47, \quad Sh_0 = 0.25, \quad Re_0 = 1022.$$

Note that these quantities are in good agreement with measured data [8, 13]. Moreover, numerical calculations show that the derivatives of the computed quantities remain of order one.

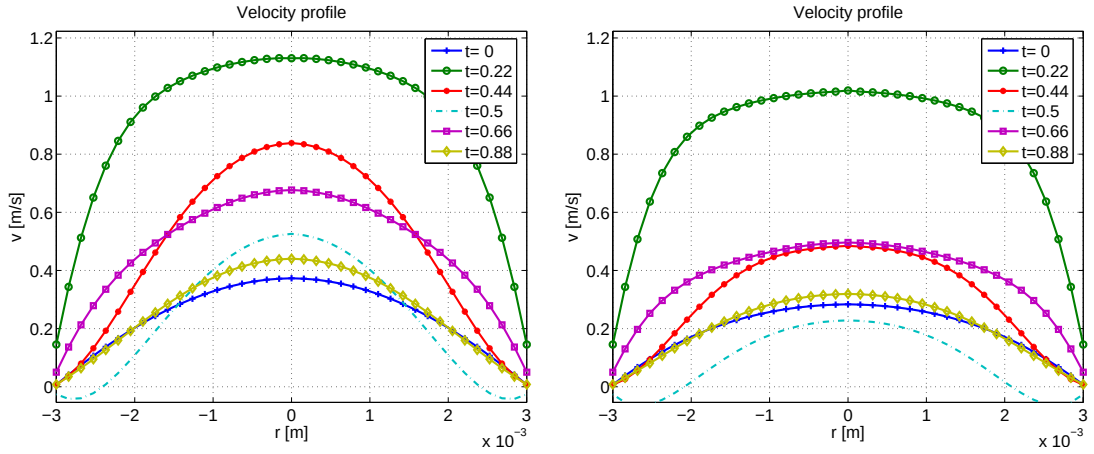

Figure 5: Velocity profiles for different times in one cardiac cycle for $slope = 10^{-7}$ (left) and $slope = 2 \cdot 10^{-4}$ (right).

The velocity decreases as the slope given in (6.2) because the resistance of the system grows (see Figure 5 and Figure 6). A local recirculation area for $t = 0.5$ is observed. The area of flow recirculation grows as the slope increases. The same property is observed while decreasing the radius of the tube with constant radius.

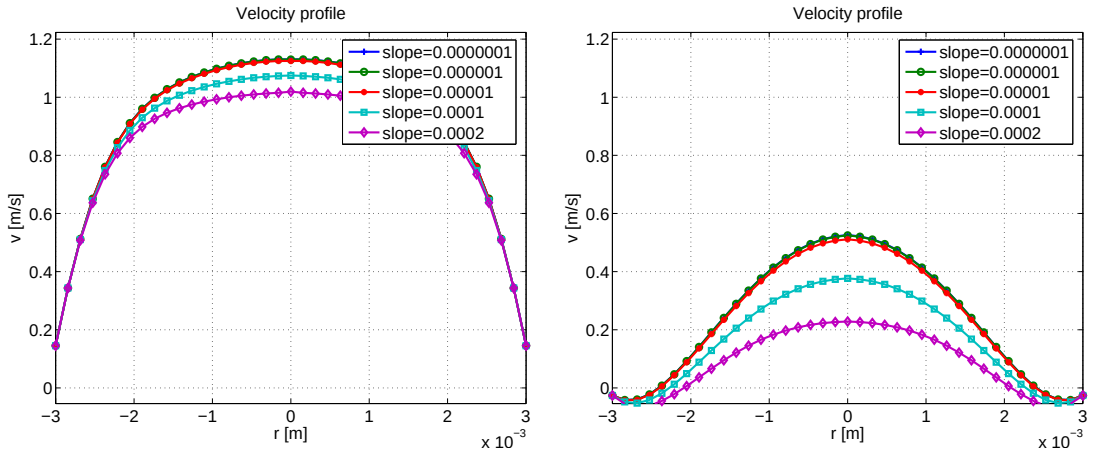

Figure 6: Velocity profiles for different *slopes* at time $t = 0.22s$ (left) and time $t = 0.5s$ (right) in one cardiac cycle.

The solution of the model for slope 10^{-7} practically corresponds to the tube of constant radius (see Figure 7) as well as the solutions for slopes 10^{-6} and 10^{-5}. As the radius of the tapered tube is decreased the velocity grows from the inlet to the outlet.

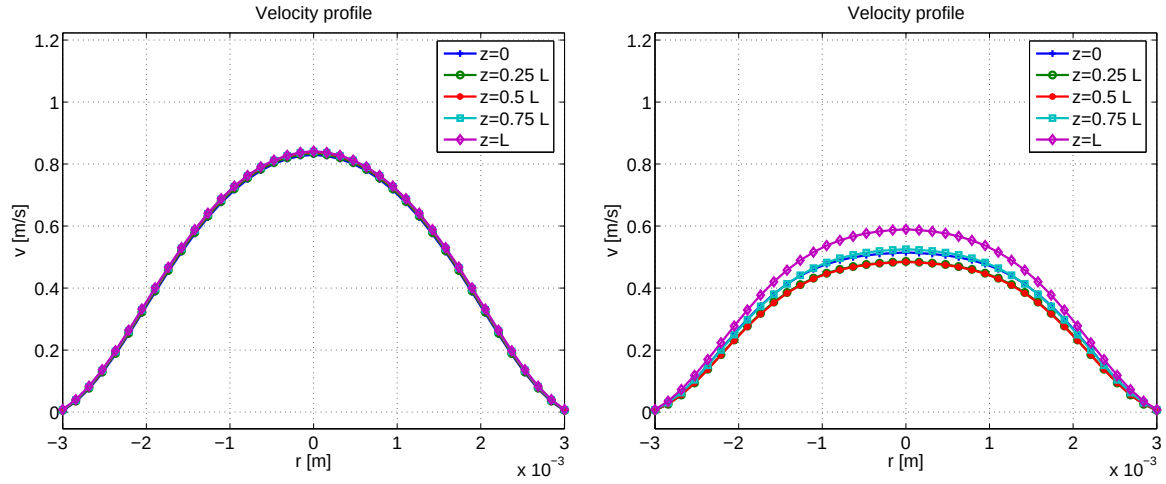

Figure 7: Velocity profiles for different longitudinal cross–section and $slope = 10^{-7}$ (left) and $slope = 2 \cdot 10^{-4}$ (right) at time $t = 0.44$.

References

[1] Auriault, J.-L., *Poroelastic media*, in: U. Hornung (ed.): Homogenization and

Porous Media, Interdisciplinary Applied Mathematics, Springer, Berlin, (1997), 163-182.

[2] Ciarlet, P.G., *Mathematical elasticity. Vol. III. Theory of shells.* Studies in Mathematics and its Applications *29*.

[3] Ciarlet, P.G. and Lods, V., *Asymptotic analysis of linearly elastic shells. I. Justification of membrane shell equations.* Arch. Rational Mech. Anal. *136* (1996), 119–161.

[4] Čanić, S. and Mikelić, A., *Effective equations modeling the flow of a viscous incompressible fluid through a long elastic tube arising in the study of blood flow through small arteries.*, SIAM Journal on Applied Dynamical Systems *2* (2003), 431–463.

[5] Čanić, S., Mikelić, A., Lamponi, D. and Tambača, J., *Self-Consistent Effective Equations Modeling Blood Flow in Medium-to-Large Compliant Arteries.* Multiscale Modeling and Simulation *3* (2005), 559–596.

[6] Čanić, S., Mikelić, A. and Tambača, J., *A two-dimensional effective model describing fluid-structure interaction in blood flow: analysis, simulation and experimental validation* Special Issue of Comptes Rendus Mechanique Acad. Sci. Paris, to appear.

[7] Fung, Y.C., *Biomechanics*: *Circulation*, Springer, New York, 1993.

[8] Kröger, K., Massalha, K., Buss, C. and Rudofsky, G., *Effect of hemodynamic conditions on sonographic measurements of peak systolic velocity and arterial diameter in patients with peripheral arterial stenosis* Journal of Clinical Ultrasound *28* , 109-114.

[9] Luchini, P., Lupo, M. and Pozzi, A., *Unsteady Stokes flow in a distensible pipe.* Z. Angew. Math. Mech. *71* (1991), 367–378.

[10] Ma, X., Lee, G.C. and Wu., S.G. *Numerical simulation for the propagation of nonlinear waves in arteries*. Transactions of the ASME *114* (1992), 490–496.

[11] Nichols, W. W. and O'Rourke, M. F., *McDonald's Blood Flow in Arteries*: *Theoretical, experimental and clinical principles, Fourth Edition*, Arnold and Oxford University.

[12] Quarteroni, A., Tuveri, M. and Veneziani, A., *Computational vascular fluid dynamics*: *problems, models and methods. Survey article*, Comput. Visual. Sci. *2* (2000), 163–197.

[13] Taylor, C.A., Hughes, T.J.R. and Zarins, C.K., *Effect of Exercise on Hemodynamic Conditions in the Abdominal Aorta*. Journal of Vascular Surgery, *29* (1999), 1077-1089.

Josip Tambača
Departament of Mathematics
University of Zagreb
Bijenička 30
10000 Zagreb, Croatia
e-mail: *tambaca@math.hr*

Sunčica Čanić
Department of Mathematics
University of Houston
4800 Calhoun Rd.,
Houston TX 77204-3476, USA
e-mail: *canic@math.uh.edu*

Andro Mikelić
LaPCS, UFR Mathématiques
Université Claude Bernard Lyon 1
21, bd. Claude Bernard
69622 Villeurbanne Cedex, France
e-mail: *mikelic@univ-lyon1.fr*